Energy Conversion
Circuit Laboratory

# Novel Burst-mode Control Strategy for Enhanced Light-load Efficiency of DAB Converters

Byeong-Ryeol Na*, Jeong-Soo Park**, Chanh-Tin Truong***, Sung-Jin Choi****
*Department of Electrical, Electronic and Computer Engineering*
*University of Ulsan, Ulsan 44610, Republic of Korea*
bulesky503@naver.com*, joungsu1127@gmail.com**, chanhtin990@gmail.com***, sjchoi@ulsan.ac.kr****

***Abstract*—Dual active bridge (DAB) converter is widely used in many applications. Nonetheless, it's efficiency degrades significantly under light-load conditions due to the high switching and conduction losses. Since a detailed analysis for burst-mode design has not been presented in the literature the effective burst-mode control for the light-load condition is proposed in this paper. In the proposed burst-mode, the regular duty and the burst duty are optimally coordinated to achieve the zero-voltage-switching (ZVS) condition and the minimum backflow power at the same time. Moreover, DC bias current is effectively eliminated in the proposed burst-mode. Therefore, the switching loss and conduction loss are simultaneously minimized, thus the light-load efficiency is significantly improved. The detailed analysis and design procedure are also presented. The 4 kW DAB converter prototype is built to verify the proposed method and the experiment results show about 2 % of increment in efficiency of the proposed method compared to the conventional burst-mode method.**

***Index Terms*—Dual active bridge converter, burst-mode, optimal backflow- power, efficiency, light-load condition, ZVS condition.**

## I. Introduction

The isolated dual-active-bridge (DAB) converter is one of the most popular converters in applications such as solid-state transformers, multi-input converters, and other applications due to its bidirectional and symmetrical structure, zero-voltage-switching (ZVS), and wide voltage gain regulation capabilities [1]–[3]. These features allow it to be used in systems such as energy storage systems and uninterruptible power supplies, which are characterized by continuously fluctuating output voltage conditions from renewable energy sources or batteries and variable loads. These characteristics necessitate high efficiency over a wide range of effective input-output voltage ratios, particularly under light-load conditions.

The single-phase-shift (SPS) control for DAB converters is the simplest modulation method for DAB control strategies used by industry practitioner due to its low cost, simple implementation, and easy design [4]. However, SPS control of DAB increases backflow power under light-loads, generating circulating currents [5], [6]. To overcome this limitation, many modulation controls such as Extended-phase-shift (EPS), Dual-phase-shift (DPS), and Triple-phase-shift (TPS) have been proposed [7]–[9]. However, the complexity of control strategies with many control variables makes optimal control difficult. Furthermore, if the voltage gain is not unity in light-load conditions, hard switching occurs, resulting in reduced efficiency [10]. Although additional magnetizing inductance is used to achieve full-range ZVS and improve light-load efficiency of the DAB converter, this is not recommended due to increased size, cost, and losses in some sections [11].

To address the two main issues of SPS control under light-load operation of the DAB, burst-mode is widely used. Burst-mode significantly reduces dependent losses such as conduction loss, switching loss, and core loss [12]. Recently, burst-mode has been applied to DAB converters to improve light-load efficiency. The design of burst-mode parameters, such as burst-mode frequency and burst-mode duty cycle, is presented in [13]. Small-signal modeling for burst-mode control is presented in [14]. However, DC bias current occurs at every first cycle of burst-mode operation, which can cause inductor current spikes and over saturation of transformer in conventional burst-mode [15]–[17].

To improve the performance of the burst-mode, the optimal burst-mode control for the light-load condition is proposed in this paper. In the proposed method the optimal duty is adaptively calculated in the burst-mode control to minimize the backflow power while the burst duty is used for regulating the output voltage. Moreover, DC bias current is effectively eliminated in the proposed burst-mode. The advantages of the proposed burst-mode can be listed as follows:

1) No additional components are needed for efficiency improvement at light-load condition.
2) The ZVS is achieved for entire load range.
3) Backflows power is minimized at the light-load condition.
4) DC bias current elimination is applied for the burst-mode.
5) Mode switching algorithm between the burst-mode and normal-mode is proposed.

This paper is structured as follows: Section II discusses the operation of DAB converter, and Section III presents the proposed burst-mode for DAB converter. The analysis is verified by experiment in Section V. Finally, the results of the study are summarized in Section VI.

This work was supported by the National Research Foundation of Korea (NRF) grant funded by the Korea government (MSIT) (RS-2023-00240194) and by the Regional Innovation Strategy (RIS) through the National Research Foundation of Korea (NRF), funded by the Ministry of Education (MOE) (2021RIS-003).

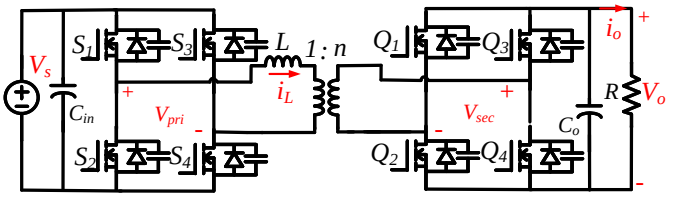


Fig. 1: Isolated DAB converter.

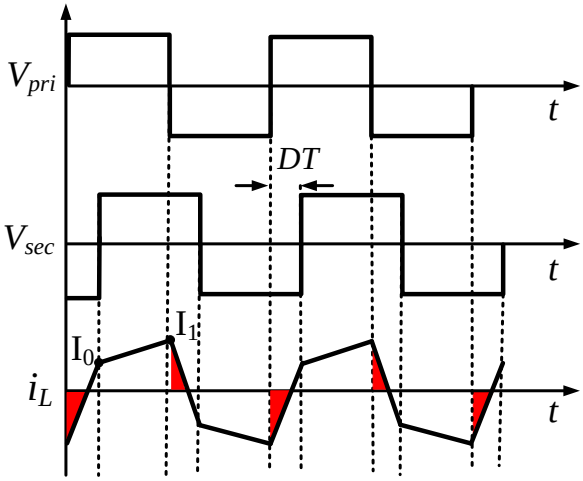


(a)

Fig. 2: Key operation waveforms of the DAB converter with SPS.

## II. Operation of the Isolated DAB Converter

Fig. 1. shows DAB converter circuit that has two active full-bridge to generate the square wave, a series inductor $L$ to store energy for power transfer, and a transformer with turn ratio $1:n$ to meet the high voltage ratio and provide the galvanic isolation. The key waveform with SPS of DAB converter is shown in Fig. 2, where the currents at the vertices are given by

$$I_o = \left[V_s + \frac{V_o}{n}(2D-1)\right]\frac{T_s}{4L} \tag{1}$$
$$I_1 = \left[V_s(2D-1) + \frac{V_o}{n}\right]\frac{T_s}{4L}.$$

According to the analysis in [6], [10], the voltage gain $M$ and the output power $P_o$ of DAB converter are given by

$$M = \frac{V_o}{nV_s} = \frac{D(1-D)T_sR_L}{2Ln^2} \tag{2}$$

$$P_o = \frac{V_sV_oD(1-D)}{2nf_sL} \tag{3}$$

where $D$, $T_s$, and $R_L$ are the regular duty cycle, the switching period, and the load resistance. $V_s$ and $V_o$ are the input voltage and the output voltage of DAB converter. The current causing

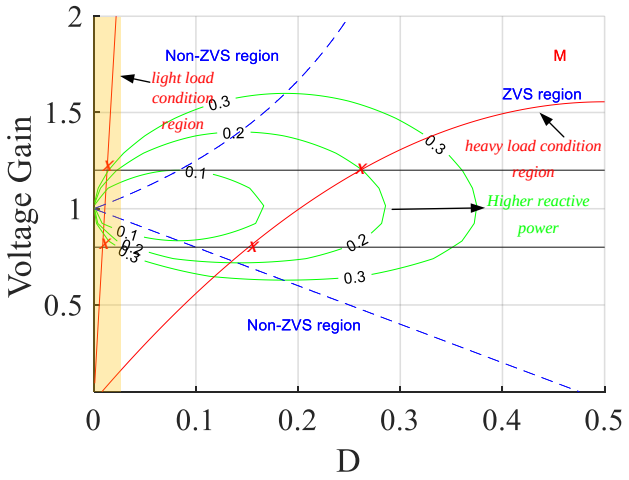


Fig. 3: ZVS condition and backflows power for different voltage gains and load conditions.

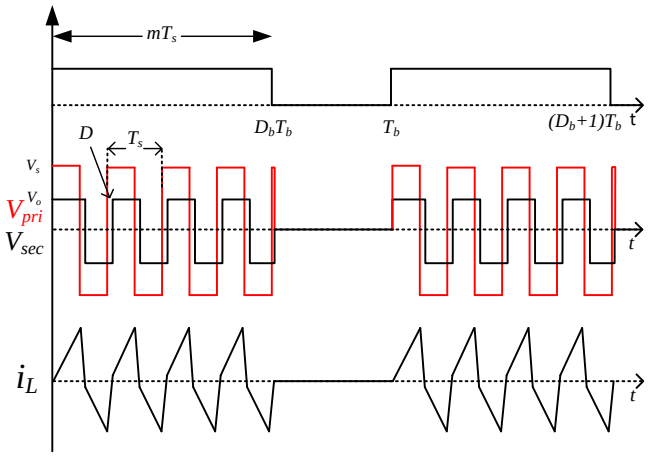


Fig. 4: Burst-mode operation waveform.

backflow power $Q$ of DAB converter are shown in the red area in Fig. 2 and its formula are given by

$$\begin{cases} Q = \frac{nV_sV_o[M+(2D-1)]^2}{16f_sL(M+1)} & nV_s \le V_o \\ Q = \frac{nV_sV_o\left[\frac{1}{M}+(2D-1)\right]^2}{16f_sL\left(\frac{1}{M}+1\right)} & nV_s > V_o. \end{cases} \tag{4}$$

The ZVS condition of DAB converter are given by

$$\begin{cases} D > \frac{1}{2}(1-M) & nV_s \le V_o \\ D > \frac{1}{2}\left(1-\frac{1}{M}\right) & nV_s > V_o. \end{cases} \tag{5}$$

The ratio of the backflow power to the real power and ZVS condition are plotted in the $M$-$D$ plane of Fig. 4. It should be noted that the operating point moves into the non-ZVS region with high backflow power as the load decreases. Therefore, system efficiency is significantly reduced at light-load condition for SPS of DAB converter.

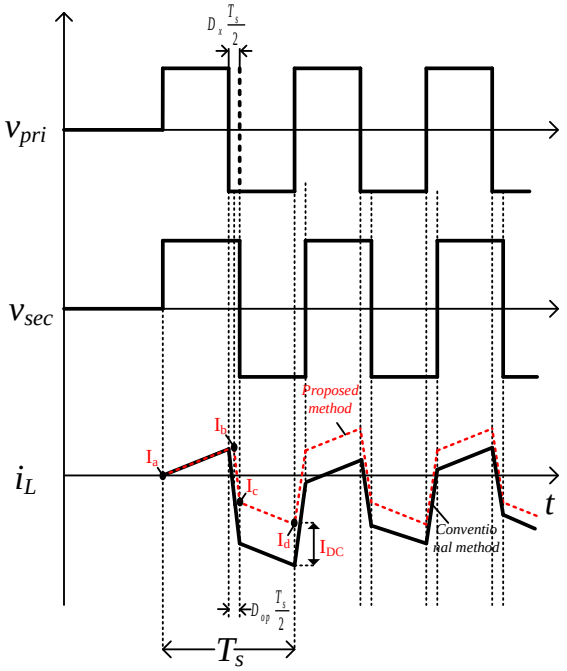


Fig. 5: DC bias elimination key waveform of the proposed burst-mode control.

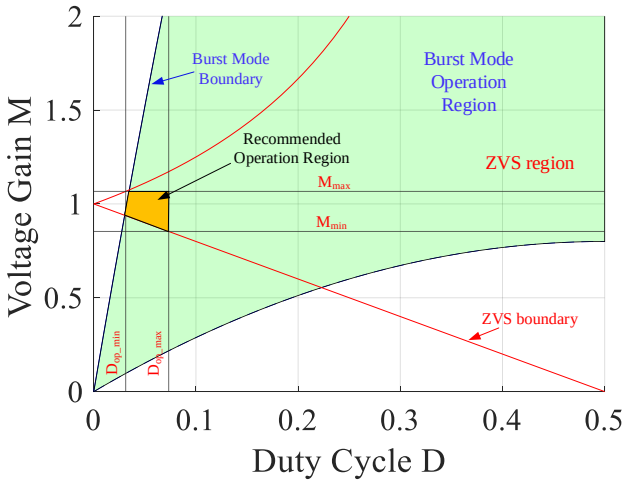


Fig. 6: Determination of the operation region for proposed burst-mode control.

## III. Proposed Burst-Mode

### A. Burst-Mode Operation

In this burst-mode operation, the PWM signal will be turned on with the burst-mode period $T_b$ and the burst duty $D_b$ is used as a control variable for regulating the output voltage $V_o$ as shown in Fig. 4. When the burst-mode is applied to in DAB converter, the voltage gain can be expressed as

$$M_b = MD_b = \frac{D(1-D)T_sR_L}{2Ln^2}D_b. \tag{6}$$

It should be noted that the output voltage can be regulated by either the regular duty cycle, $D$ or the burst-mode duty cycle, $D_b$ as shown in Fig. 6.

To minimize the backflow power in the burst-mode, the DAB converter should be operated at the optimally calculated duty cycle $D_{op}$. The optimal duty cycle $D_{op}$ for the minimum backflow power of DAB converter can be fond and when backflow power in (4) is set to zero. As such, the optimal duty cycle $D_{op}$ can be expressed as

$$\begin{cases} D_{op} = \frac{1}{2}(1-M_b) & nV_s \le V_o \\ D_{op} = \frac{1}{2}\left(1-\frac{1}{M_b}\right) & nV_s > V_o. \end{cases} \tag{7}$$

While the minimum backflow power in burst-mode is achieved by $D_{op}$, the output voltage can be regulated by $D_b$. Accordingly the updated voltage gain formula $M_b$ can be given by

$$M_b = \frac{D_{op}(1-D_{op})T_sR_L}{2Ln^2}D_b. \tag{8}$$

### B. DC Bias elimination

In the burst-mode operation, the series inductor current $i_L$ jumps from zero to the burst-mode current. In this case, DC bias current $I_{DC}$ occurs as shown in Fig. 5 which may cause the transformer saturation [15], [16]. To eliminate DC bias current, the additional duty cycle $D_x$ can be added to the optimal regular duty $D_{op}$ to cancel this effect. In the burst-mode operation, the vertex value of the series inductor current $i_L$ can be expressed as follows: $(nV_s > V_o)$

$$\begin{aligned} I_a &= 0 \\ I_b &= I_a + \frac{nV_s - V_o}{L}(1+D_{op})\frac{T_s}{2} \\ I_c &= I_b + \frac{nV_s + V_o}{L}D_x\frac{T_s}{2} \\ I_d &= I_c + \frac{V_o - nV_s}{L}(1-D_x)\frac{T_s}{2}. \end{aligned} \tag{9}$$

By arranging (9),

$$I_{DC} = (D_{op}(nV_s - V_o) + 2D_xnV_s)\frac{T_s}{2L} \quad nV_s > V_o. \tag{10}$$

To nullify $I_{DC}$, the value of $I_d$ should meet the following condition:

$$I_d = \frac{-nV_s + V_o(1-2D_{op})}{4}\frac{T_s}{L} \quad nV_s > V_o. \tag{11}$$

By substituting (11) to (9), the value of $D_x$ for zero bias current is given by

$$D_x = \frac{1}{4}(M - 2D_{op} - 1) \quad nV_s > V_o \tag{12}$$

In order not to disturb the optimal duty operation, the regular duty cycle is applied only for the first pulse of each burst-mode cycle, and its formula is given by

$$D'_n = D_{op} + D_x. \tag{13}$$

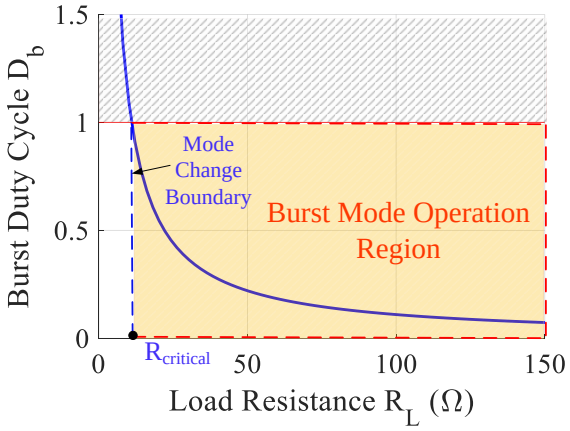


Fig. 7: Critical load value $R_{critical}$ for mode change condition.

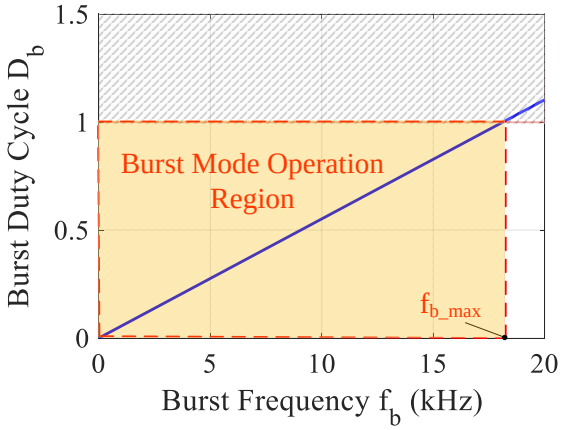


Fig. 8: The burst-mode duty cycle $D_b$ versus burst frequency $f_b$.

## IV. Design Procedure

According to the analysis of the Section II the design procedure is established in this section. From the updated voltage gain formula in (8), it can be realized that when the duty cycle $D$ is fixed at optimal duty cycle $D_{op}$ for the minimum backflow power, the burst duty cycle $D_b$ should be used to regulate output voltage, and it is given by

$$D_b = \frac{2M_bLn^2}{D_{op}(1-D_{op})T_sR_L}. \tag{14}$$

The burst-mode duty cycle $D_b$ is a function of the load resistance $R_L$. It is well known that the range of the burst duty cycle is $0 \leq D_b \leq 1$. Therefore, the critical load value $R_{critical}$ for the mode switching between the burst-mode and the normal mode of DAB converter is determined as shown in Fig. 7 and its formula is given by

$$R_{critical} = \frac{2M_bLn^2}{D_{op}(1-D_{op})T_s}. \tag{15}$$

By the way the output capacitor filter $C_o$ plays very importance role in the burst-mode. Because the power is directly supplied from $C_o$ to load under the burst-mode, the maximum allowable output voltage ripple $\Delta V_{max}$ is directly related to capacitance value of $C_o$ as shown

$$C_o = \frac{I_o}{\Delta V_o f_b}. \tag{16}$$

By substituting (16) into (14), the burst duty cycle $D_b$ can be rewritten as follows:

$$D_b = \frac{2M_bLn^2}{D_{op}(1-D_{op})T_s}\frac{f_bC_o\Delta V_o}{V_o}. \tag{17}$$

It should be noted that with given the maximum allowable output voltage ripple $\Delta V_{max}$, the higher $f_b$ would lead to the smaller $C_o$. The burst-mode duty cycle $D_b$ versus burst frequency $f_b$ can be plotted as shown in Fig. 8. Therefore, the burst-mode frequency is also determined. The design process of the proposed burst-mode is as follows:

1) The initial system parameters such as $V_s$, $V_o$, $P_o$ $f_s$, $f_b$, and $\Delta V_{max}$ are given by the system requirement.
2) The voltage gain $M_b$ and the optimal duty cycle $D_{op}$ can be calculated by (2) and (7).
3) The value of inductance $L$ can be calculated by (3).
4) The critical load resistance value $R_{critial}$ is calculated by (15) and (17).
5) Output voltage $C_o$ is calculated by (16) then design procedure is repeated from step 4. Otherwise the design procedure is finished.

TABLE I: System parameters.

| Symbol | Parameters | Values | Unit |
|---|---|---|---|
| $V_s$ | DC input voltage | 400 | V |
| $V_o$ | DC output voltage | 100-180 | V |
| $f_s$ | Switching frequency | 50 | kHz |
| $P_o$ | Output power | 0-4 | kW |
| $n$ | Transformer turns ratio | 0.5 | |
| $C_o$ | Output filter capacitance | 500 | $\mu$F |
| $L$ | Series inductance | 50 | $\mu$H |
| $f_b$ | Burst frequency | 2.5 | kHz |
| $R_{critial}$ | Critical value of load resistance | 50 | Ω |

## V. Experimental Verification

To verify the proposed control strategy, a 4 $kW$ DAB converter prototype was built as shown in Fig. 9. The design procedure in Section IV is applied to design the system parameters shown in Table I. DSP (TMS320F28335 from Texas Instruments) is used as the digital controller for algorithm implementation. MOSFET module(F4-17MR12W1M1H B76) is used for main power switches. A power analyzer (Yokogawa Electric, WT1804E) is used for efficiency measurement. Several experimental tests are conducted to verify the performance of the proposed burst-mode control, which was performed with buck type.

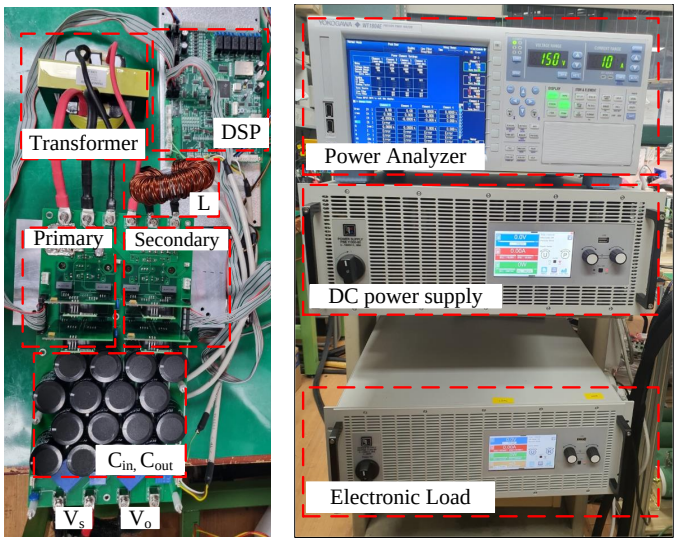


(a) (b)

Fig. 9: Experimental setup: (a) prototype DAB converter (b) DC power supply, electronic load, and measurement equipment.

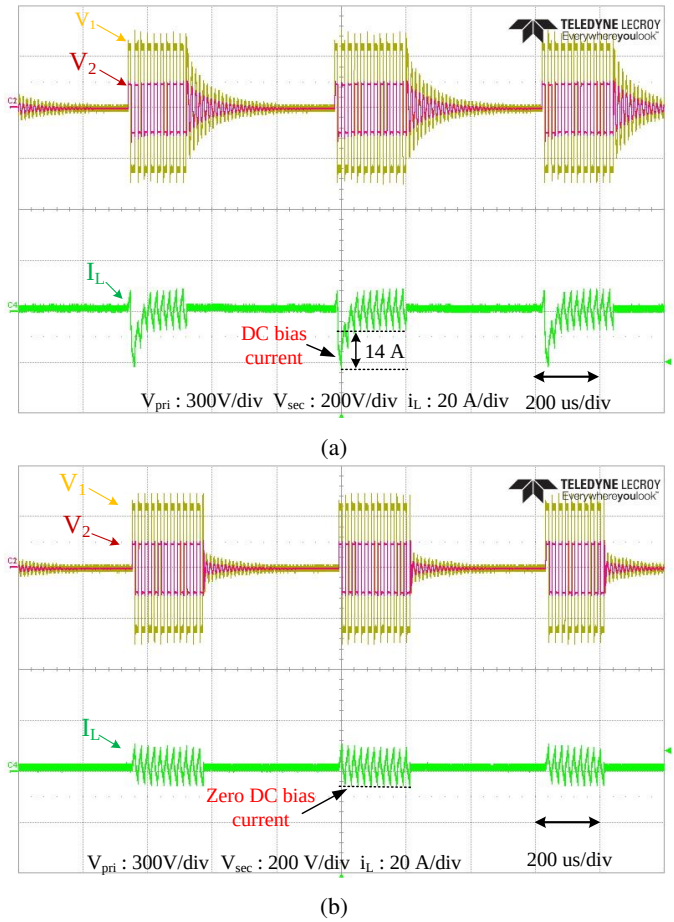


(a)

(b)

Fig. 10: Experimental waveforms of DC bias elimination (a) conventional burst-mode (b) proposed burst-mode.

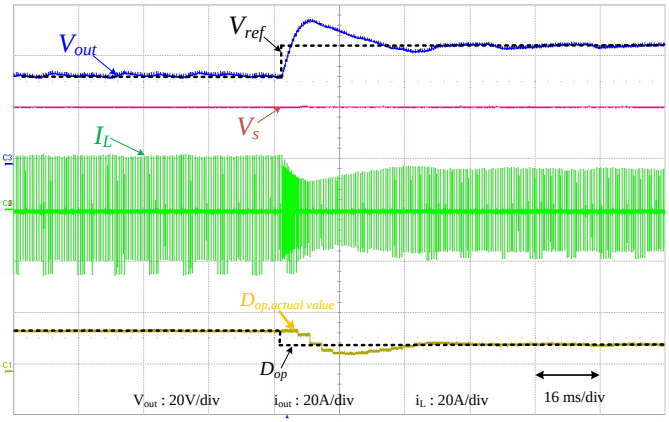


Fig. 11: Experimental waveforms of the proposed burst-mode control when $V_{ref}$ changes from 90 $V$ to 120 $V$.

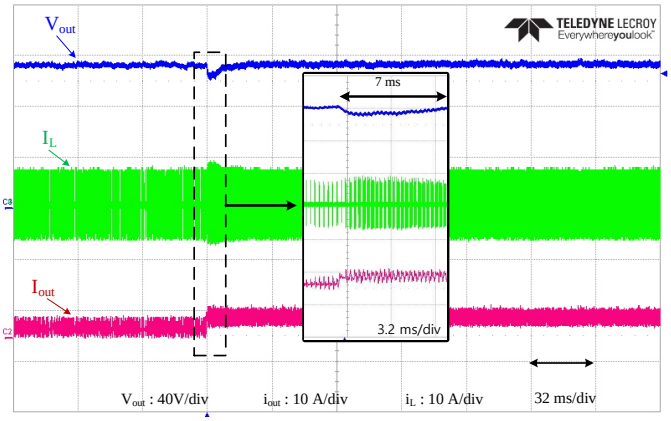


Fig. 12: Experimental waveforms of DAB converter of the proposed burst-mode control when load changes from 80 Ω to 40 Ω.

In case of the conventional burst-mode without DC bias elimination, there is 14 $A$ DC at staring up the PWM of the burst-mode as shown in Fig. 10a. In the proposed method, after the DC bias current elimination is activated, there is zero bias current as shown in Fig. 10b.

The step change of output voltage $V_o$ is also tested when $V_{ref}$ steps up from 90 $V$ to 120 $V$. The output voltage $V_o$ can be regulated well with the reference value. Moreover, the optimal duty cycle $D_{op}$ is changed from 0.275 to 0.2 when the $V_o$ is increased from 90 $V$ to 120 $V$, which matches well with calculation value in Fig. 11.

The current is increased from 1.5 $A$ to 3 $A$ when the load resistance is changed from 80 Ω to 40 Ω when The undershoot of the output voltage is 4 $V$, which is 4 % of the steady-state output voltage as shown in Fig. 12.

The mode switching operation of the proposed control strategy is tested: burst-mode to normal mode and normal mode to burst-mode. In the case of burst-mode to normal mode, the load resistance is reduced from 80 Ω to 40 Ω when the output current changes from 1.5 $A$ to 3 $A$. During the mode switching the output voltage can be regulated with a

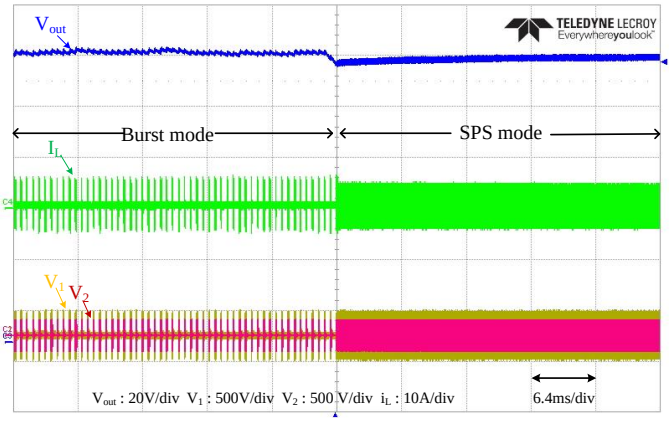


(a)

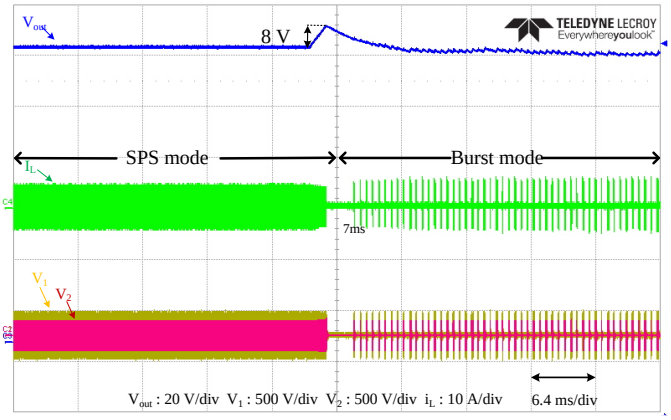


(b)

Fig. 13: Experimental waveforms of the mode switching (a) from burst-mode to normal-mode (b) from normal-mode to burst-mode.

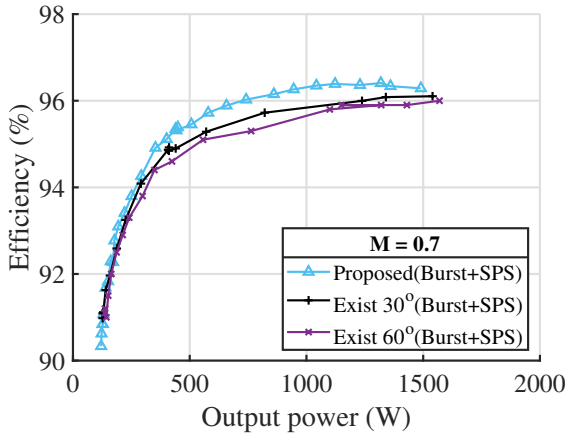


(a)

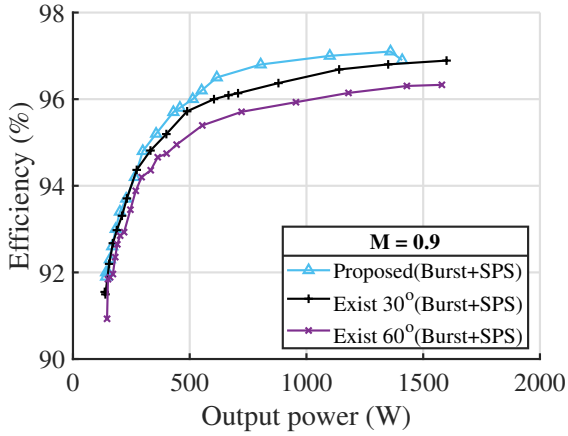


(b)

Fig. 14: Efficiency measurement comparison for a) $M = 0.7$ b) $M = 0.9$.

slight undershoot as shown in Fig. 13a. Moreover, in the case from normal-mode to burst-mode, when the load resistance is increased from 40 Ω to 80 Ω, the output current changes from 3 $A$ to 1.5 $A$. During the mode change the output voltage can be regulated with a slight overshoot as shown in Fig. 13b.

The efficiency of the proposed method is compared with conventional burst-mode as shown in Fig. 14. Due to the ZVS operation and minimum backflows power, the efficiency of the proposed method is much higher than conventional method in entire load condition.

## VI. Conclusion

In this paper, the burst-mode for SPS-modulation DAB converter is proposed. The DAB converter is operated at minimum backflow power condition as well as ZVS at light-load condition. Therefore, the system efficiency is significantly improved. The DC bias current issue of conventional burst-mode is also mitigated in the proposed method. The detailed design procedure of DAB converter for burst-mode control is also presented. The effectiveness of proposed burst-mode is verified by experiment. System efficiency can be improved by 2 % compared with the conventional burst-mode method.

## References


[1] M. Kheraluwala, R. Gascoigne, D. Divan, and E. Baumann, "Performance characterization of a high-power dual active bridge dc-to-dc converter," *IEEE Transactions on Industry Applications*, vol. 28, no. 6, pp. 1294–1301, 1992.

[2] B. Zhao, Q. Song, W. Liu, and Y. Sun, "Overview of dual-active-bridge isolated bidirectional dc–dc converter for high-frequency-link power-conversion system," *IEEE Transactions on Power Electronics*, vol. 29, no. 8, pp. 4091–4106, 2014.

[3] R. De Doncker, D. Divan, and M. Kheraluwala, "A three-phase soft-switched high-power-density dc/dc converter for high-power applications," *IEEE Transactions on Industry Applications*, vol. 27, no. 1, pp. 63–73, 1991.

[4] X. Chen, G. Xu, H. Han, D. Liu, Y. Sun, and M. Su, "Light-load efficiency enhancement of high-frequency dual-active-bridge converter under sps control," *IEEE Transactions on Industrial Electronics*, vol. 68, no. 12, pp. 12 941–12 946, 2021.

[5] H. Bai and C. Mi, "Eliminate reactive power and increase system efficiency of isolated bidirectional dual-active-bridge dc–dc converters using novel dual-phase-shift control," *IEEE Transactions on Power Electronics*, vol. 23, no. 6, pp. 2905–2914, 2008.

[6] H. Shi, H. Wen, J. Chen, Y. Hu, L. Jiang, G. Chen, and J. Ma, "Minimum-backflow-power scheme of dab-based solid-state transformer with extended-phase-shift control," *IEEE Transactions on Industry Applications*, vol. 54, no. 4, pp. 3483–3496, 2018.

[7] B. Zhao, Q. Yu, and W. Sun, "Extended-phase-shift control of isolated bidirectional dc–dc converter for power distribution in microgrid," *IEEE Transactions on Power Electronics*, vol. 27, no. 11, pp. 4667–4680, 2012.
[8] H. Bai, Z. Nie, and C. C. Mi, "Experimental comparison of traditional phase-shift, dual-phase-shift, and model-based control of isolated bidirectional dc–dc converters," *IEEE Transactions on Power Electronics*, vol. 25, no. 6, pp. 1444–1449, 2010.
[9] J. Huang, Y. Wang, Z. Li, and W. Lei, "Unified triple-phase-shift control to minimize current stress and achieve full soft-switching of isolated bidirectional dc–dc converter," *IEEE Transactions on Industrial Electronics*, vol. 63, no. 7, pp. 4169–4179, 2016.
[10] A. R. Rodríguez Alonso, J. Sebastian, D. G. Lamar, M. M. Hernando, and A. Vazquez, "An overall study of a dual active bridge for bidirectional dc/dc conversion," in *2010 IEEE Energy Conversion Congress and Exposition*, 2010, pp. 1129–1135.
[11] Y. P. Chan, K. H. Loo, M. Yaqoob, and Y. M. Lai, "A structurally reconfigurable resonant dual-active-bridge converter and modulation method to achieve full-range soft-switching and enhanced light-load efficiency," *IEEE Transactions on Power Electronics*, vol. 34, no. 5, pp. 4195–4207, 2019.
[12] W. Feng, F. C. Lee, and P. Mattavelli, "Optimal trajectory control of burst mode for llc resonant converter," *IEEE Transactions on Power Electronics*, vol. 28, no. 1, pp. 457–466, 2013.
[13] Y. Yao, G. S. Kulothungan, and H. S. Krishnamoorthy, "Improved circuit design and adaptive burst mode control in psfb converters for higher efficiency over a wide power range," *IEEE Access*, vol. 10, pp. 9152–9163, 2022.
[14] V. M. Iyer, S. Gulur, and S. Bhattacharya, "Hybrid control strategy to extend the zvs range of a dual active bridge converter," in *2017 IEEE Applied Power Electronics Conference and Exposition (APEC)*, 2017, pp. 2035–2042.
[15] Q. Bu, H. Wen, H. Shi, and Y. Zhu, "A comparative review of high-frequency transient dc bias current mitigation strategies in dual-active-bridge dc–dc converters under phase-shift modulations," *IEEE Transactions on Industry Applications*, vol. 58, no. 2, pp. 2166–2182, 2022.
[16] B. Zhao, Q. Song, W. Liu, and Y. Zhao, "Transient dc bias and current impact effects of high-frequency-isolated bidirectional dc–dc converter in practice," *IEEE Transactions on Power Electronics*, vol. 31, no. 4, pp. 3203–3216, 2016.
[17] X. Li and Y.-F. Li, "An optimized phase-shift modulation for fast transient response in a dual-active-bridge converter," *IEEE Transactions on Power Electronics*, vol. 29, no. 6, pp. 2661–2665, 2014.